Dynamic cluster-size distribution in cluster-cluster aggregation: Effects of cluster diffusivity

Paul Meakin
Central Research and Development Department, Experimental Station, E. I. du Pont de Nemours and Company, Inc., Wilmington, Delaware 19898

Tamás Vicsek* and Fereydoon Family
Department of Physics, Emory University, Atlanta, Georgia 30322
(Received 24 July 1984)

The dynamics of the diffusion-limited model of cluster-cluster aggregation is investigated in two and three dimensions by studying the temporal evolution of the cluster-size distribution $n_s(t)$, which is the number of clusters of size s at time t. In a recent study it was shown that the results of the two-dimensional simulations for mass-independent diffusivity can be well represented by a dynamic-scaling function of the form $n_s(t) \sim s^{-2} f(s/t^z)$, where $f(x)$ is a scaling function with a power-law behavior for small x, namely $f(x) \sim x^\delta$ for $x \ll 1$ and $f(x) \ll 1$ for $x \gg 1$. In this paper we extend the calculations of the cluster-size distribution to three dimensions and to the case of the cluster diffusivity depending on the size of the clusters. The diffusion constant of a cluster of size s is assumed to be proportional to s^γ. The overall behavior of $n_s(t)$ and the exponents δ and z have been determined for a set of values of γ. We find that the results are consistent with the scaling theory, and the exponents in $n_s(t)$ depend continuously on γ. Moreover, there is a critical value of γ $[\gamma_c(d=2) \simeq -\frac{1}{4}, \gamma_c(d=3) \simeq -\frac{1}{2}]$ at which the shape of the cluster-size distribution crosses over from a monotonically decreasing function to a bell-shaped curve which can be described by the above scaling form for $n_s(t)$, but with a scaling function $\tilde{f}(x)$ different from $f(x)$.

I. INTRODUCTION

The main process in many phenomena of practical importance in physics, chemistry, biology, medicine, and engineering is the formation of clusters by aggregation of particles or the clusters themselves.[1] A widely used method of describing such systems is the determination of the cluster-size distribution function.[2,3] This quantity describes the dependence of the number of clusters on their mass, which is measured in experiments[4–8] and is the focus of a kinetic-equation approach to coagulation.[9,10]

Diffusion-limited aggregation of clusters can be well modeled by a process introduced by Meakin[11] and by Kolb *et al.*[12] In the Monte Carlo simulation of this model, diffusing particles join together upon contact to form clusters which continue diffusing and sticking together. The initial impetus for studying this model came from the fact that the large clusters formed in this process were found to have a scale-invariant, fractal structure.[13] This fractal property, which is shared by other diffusion-limited-aggregation models,[14–16] has recently become a subject of considerable interest. Much of the activity in this field has been focused on the determination of the fractal dimensionality of the clusters in various dimensions. The fractal dimensionality, however, conveys only a limited amount of information about the aggregation process. First, it is a static quantity and does not describe the dynamics of the aggregation process. Moreover, the fractal dimension refers to the geometrical properties of only one cluster and it is not useful in describing the ensemble of clusters in the system. Investigation of the dynamic cluster-size distribution function $n_s(t)$, which is the number of clusters in a unit volume consisting of s particles at time t, enables us to achieve both goals.

The study of the statistics of clusters if a common approach to the description of ensembles of clusters in the statistical mechanics of equilibrium systems.[17–20] The success of the methods developed for the treatment of continuous phase transitions has prompted the application of these ideas to nonequilibrium processes. As a result, the scaling properties of the cluster-size distribution have been studied in various nonequilibrium models. A time-dependent scaling function for the size distribution of the coagulating droplets in a quenched Ising system was discussed by Binder.[20] The decay of $n_s(t)$ as a function of the cluster size has been determined in the kinetic-gelation[21] and diffusion-controlled—deposition models.[22,23] von Schulthess *et al.*[6] measured the distribution of cluster sizes in antigens crosslinked by antibodies and observed scaling in both s and t. The second moment of the cluster-size distribution was measured by light-scattering experiments on gelation[24] and gold colloids,[25] and the results were found to scale with time. In order to determine the kinetics of the cluster-size distribution, a number of authors have used von Smoluchowski's equation,[26–30] assuming various mathematical forms for the interparticle reaction rates. In some cases[29,30] the solutions of the kinetic equation were found to behave like the experiments and the computer-simulation results. However, a quantitative comparison will only be possible if the relation between the rate constant and the dynamics of the diffusion-limited-aggregation process is known.

Very recently, a dynamic-scaling description was introduced[3,31] for the size distribution in the model of diffusion-limited aggregation of clusters. It was shown[3] that in the case when the diffusivity of the clusters does not depend on their mass, the results of the two-dimensional Monte Carlo simulations can be well represented by a dynamic-scaling function for $n_s(t)$ of the form

$$n_s(t) \sim s^{-2} f(s/t^z) , \tag{1}$$

where $f(x)$ is a scaling function with a power-law behavior for small x, namely $f(x) \sim x^{\delta}$ for $x \ll 1$, and $f(x) \ll 1$ for $x \gg 1$. Equation (1) was assumed to be valid for small densities of the the particles and for $s,t \gg 1$. According to (1) for $s/t^z \ll 1$, $n_s(t) \sim t^{-2} s^{-\tau}$ with $w = z\delta$ and $\delta = 2-\tau$, i.e., the cluster-size distribution decreases as a power law in s and t and the exponents satisfy the scaling relation $w = (2-\tau)z$. For $s/t^z \gg 1$, $n_s(t)$ decays faster than any power of its argument.

An immediate consequence of the scaling form (1) is that the mean cluster size $S(t) = \sum s^2 n_s(t)$ diverges as $t \to \infty$. Expressing $S(t)$ in terms of $n_s(t)$ and using (1), we find[3,32]

$$S(t) \sim t^z . \tag{2}$$

Another consequence of the scaling form (1) is that the total number of clusters in a unit volume $n(t) = \sum n_s(t)$ also scales with time. Using expression (1) we find[32]

$$n(t) \sim \begin{cases} t^{-z}, & \tau < 1 \\ t^{-w}, & \tau > 1 . \end{cases} \tag{3}$$

Therefore the time dependence of the total number of clusters is determined by the value of τ.

In this paper we extend the calculations of the cluster-size distribution described in Ref. 3 to three dimensions and to the case of the cluster diffusivity, depending on the size of the clusters. The diffusion constant of a cluster of size s is assumed to be proportional to s^{γ}. In Ref. 3 the case $\gamma = 0$ was considered in a two-dimensional study of the cluster-cluster—aggregation model. In the present study we determined $n_s(t)$ for $\gamma = -1.0 \to 0.5$ in $d = 2$ and $\gamma = -3.0 \to 0.5$ in $d = 3$. From the dependence of $n_s(t)$, the total number of clusters $n(t)$, and the mean cluster size $S(t)$ on t, we determine the various critical exponents and test the scaling relation proposed in Ref. 3.

The outline of the paper is as follows: In Sec. II we discuss the simulations. The results are presented in Sec. III. In Sec. IV we discuss the results and in Sec. V we present our conclusions.

II. SIMULATIONS

All of our simulations were carried out on two-dimensional square lattices or three-dimensional cubic lattices with periodic boundary conditions. Initially, $N_0 = \rho L^d$ particles are randomly placed at N_0 sites of an L^d lattice. The diffusional motion of the clusters is represented by random walks on the lattice, and clusters stick rigidly to each other on contact. In all of the models used in connection with the work described in this paper, we assume that the diffusion coefficient D_s of a cluster of mass s (where s is the number of particles in the cluster) is given by

$$D_s \sim D_0 s^{\gamma} , \tag{4}$$

where D_0 is a constant. For the case $\gamma = 0$, which corresponds to a mass-independent diffusion coefficient, clusters are selected randomly and moved by one lattice unit in a randomly chosen direction. At each move the "time" t is incremented by $1/N(t)$, where $N(t)$ is the total number of clusters in the L^d cell at time t. For the case $\gamma \neq 0$, clusters are also selected randomly. A random number x uniformly distributed in the range $0 < x < 1$ is selected and the cluster is moved only if $x < D_s/D_{\max}$, where D_s is the diffusion coefficient of the randomly selected cluster and $D_{\max}$ is the largest diffusion coefficient for any cluster in the system. After each cluster has been randomly selected, the time is incremented by $1/D_{\max}N(t)$ whether the cluster is actually moved or not. In other words the time is incremented by $D_{\max}/N(t)$ for each *attempted* move.

III. RESULTS

For all values of the diffusivity exponent γ, our three-dimensional simulations were carried out using 15 000 particles or occupied lattice sites on 100^3 lattices ($\rho = 0.015$). In most cases, simulations were also carried out using 8000 particles on 133^3 cells ($\rho = 0.0034$), and in a few cases at a density of 0.025 particles per lattice site (25 000 particles on 100^3 cells.) The time-dependent cluster-size distributions were obtained for the case $D_s \sim s^{-2}$ at a density of 0.0034 particles per lattice site. For all of the our simulations, the total number of clusters in the system $N(t)$ and the mean cluster size $S(t)$ were determined at all stages of the aggregation process [Figs. 1(a) and 1(b)]. The cluster-size distribution was also determined for clusters of various sizes as a function of time [Fig. 1(c)], and was also determined at various times [Fig. 1(d)]. For large clusters, the results for a small range of cluster sizes were averaged to obtain the results shown in Figs. 1(c) and 1(d).

The results shown in Fig. 1 exemplify the qualitative behavior for those cases where the diffusion constant exponent γ has a value smaller than about $-\frac{1}{2}$. Figure 2 shows the results of a simulation carried out with γ set to a value of $-\frac{1}{2}$ using 15 000 particles on 100^3 lattices. It can be seen from Fig. 2(a) that, at long times, the number of clusters of size s is approximately equal for all s, provided s is not too large.

Figure 3 shows the time-dependent cluster-size distributions obtained for cluster-size-independent diffusion coefficients. The results shown in this figure are typical of simulations carried out with the diffusivity exponent γ set to a value larger than $-\frac{1}{2}$. Under these conditions, $N_{s_1}(t) > N_{s_2}(t)$ at all times if $s_1 < s_2$.

Results similar to those shown in Figs. 1—3 were obtained for a number of values of γ in the range $1.0 > \gamma > -3.0$. In particular, simulations were carried

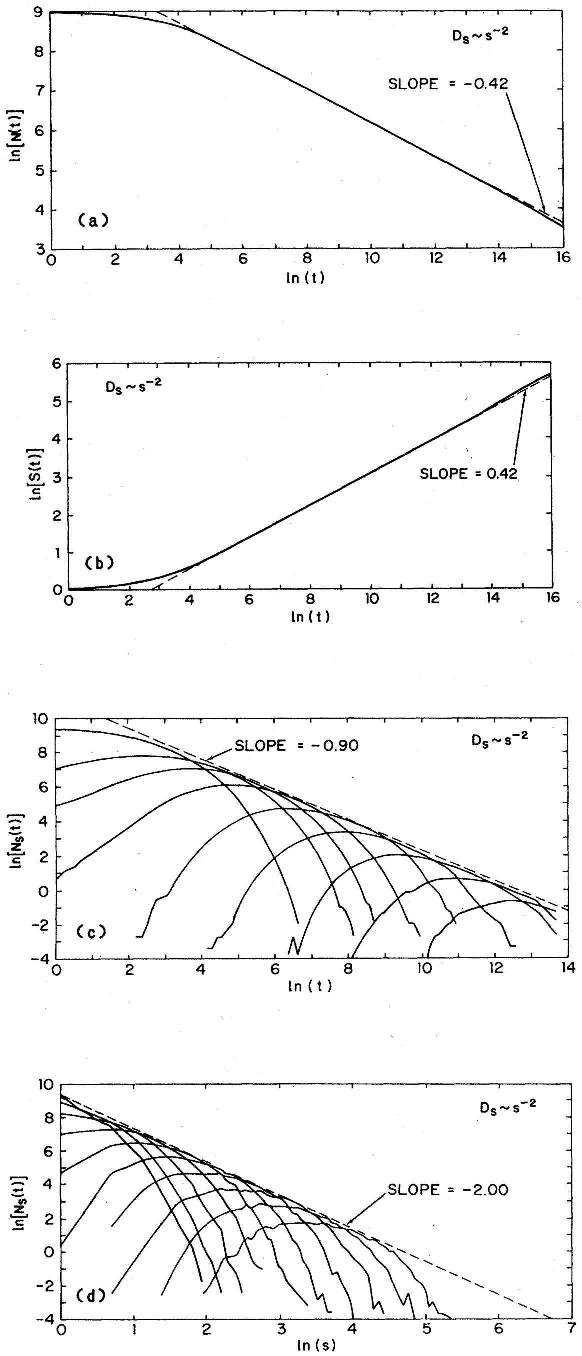

FIG. 1. Typical set of results obtained from a three-dimensional simulation of cluster-cluster aggregation. In this particular case, 8000 particles were used on 133^3 lattices, assuming that $D_s \sim s^{-2.0}$. Very similar results were obtained using 15 000 particles on 100^3 lattices. Part (a) shows the total number of clusters $N(t)$ as a function of time, and part (b) shows the mean cluster size $S(t)$. Parts (c) and (d) show the time-dependent cluster-size distribution $N_s(t)=n_s(t)L^d$, which is the number of clusters consisting of s particles at time t in the cell of linear size L. The curves in (c) correspond to cluster sizes of 1, 2, 3, 5, 10, 19–20, 38–40, 75–80, and 150–160. Part (d) shows the cluster-size distribution at the times 1.0, 4.3, 21.4, 107, 537, 2692, 1.35×10^4, 6.76×10^4, 3.39×10^5, and 1.76×10^6.

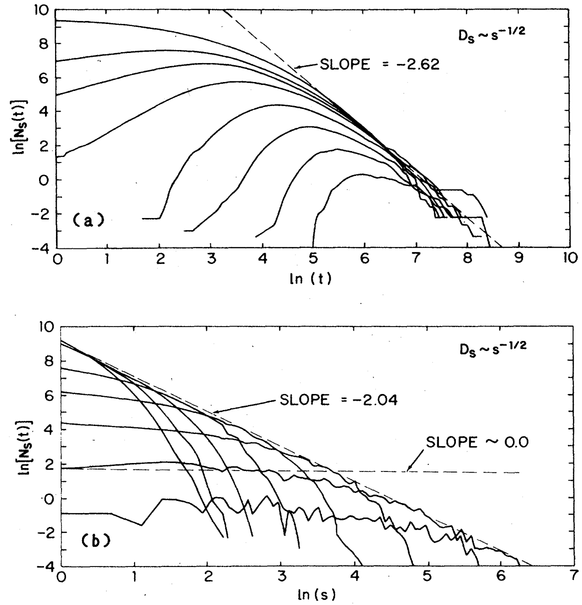

FIG. 2. Time-dependent cluster-size distributions obtained from three-dimensional simulations of cluster-cluster aggregation with a diffusivity exponent $\gamma=-\frac{1}{2}$ at a density of 0.015 particles per lattice site. Part (a) shows the number of clusters of size 1, 2, 3, 5, 10, 19–20, 38–40, 75–80, and 150–160 as a function of time during the simulation. Part (b) shows the cluster-size distribution at times 2.3, 5.8, 14.5, 36.3, 91.2, 229, 575, 1445, and 3631.

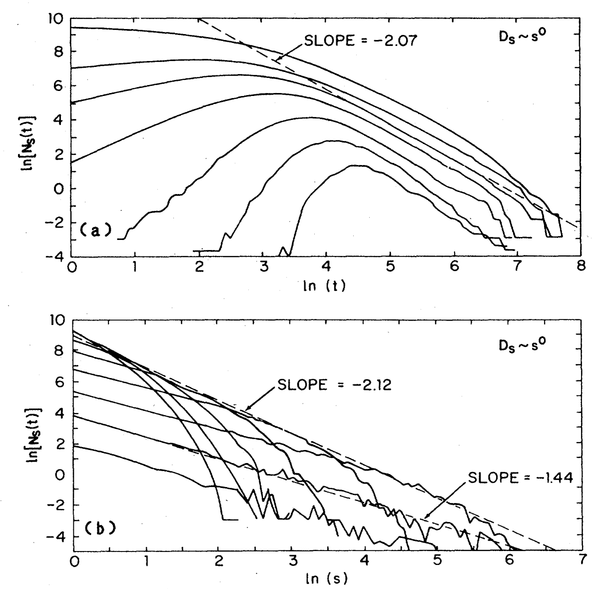

FIG. 3. Time-dependent cluster-size distributions obtained from three-dimensional simulations of cluster-cluster aggregation with size- (mass-) independent diffusion coefficients. Part (a) shows the number of clusters of size 1, 2, 3, 5, 10, 19–20, and 38–40 as a function of time, and part (b) shows the cluster-size distribution obtained at the times 2.11, 4.84, 11.1, 25.4, 133, 306, and 701. A particle density $\rho=0.015$ was used in these simulations.

TABLE I. Exponents τ, w, and z obtained from three-dimensional simulations using the expressions $n_s(t) \sim s^{-\tau} t^{-w}$ and $S(t) \sim t^z$. Note that the scaling theory predicts $w=(2-\tau)z$ for $\gamma > \gamma_c$ and $w=2z$ for $\gamma < \gamma_c$.

γ	z	w	τ	Common tangent
-3	0.33	0.64		
-2	0.45	0.90		-1.9
-1	0.8(5)	1.60		-2.0
$-1/D$	~ 1	2.2		-2.0
$-\frac{1}{2}$	$\sim 1.3-1.4$	2.6(2)	$\simeq 0$	-2.0
0	3	2.1–2.3	1.3	-2.1
$\frac{1}{2}$	(~ 100 from scaling)	12–13	1.87	-2.0

out for several values close to $-\frac{1}{2}$ to determine the critical value of γ which corresponds to the boundary between the behavior shown in Fig. 1 and that shown in Fig. 3. A parallel series of two-dimensional simulations was also carried out. Since the two-dimensional results are qualitatively similar to those obtained in three dimensions, and the three-dimensional case is of much more practical interest, only a brief summary of our two dimensional results is presented in Fig. 6.

IV. DISCUSSION

One of the most notable features of Figs. 1(d), 2(b), and 3(b) is that the envelope of the cluster-size distribution function for various times is a straight line (the common tangent) having a slope approximately equal to -2.0. This fact provides a strong support for the scaling form (1) because of the following considerations. The common tangent touches the cluster-size distribution functions in the region where the cutoff behavior of $f(x)$ appears ($x \simeq 1$); therefore, at time t_0, $s_0(t_0) \sim t_0^z$, where $s_0(t_0)$ is the s coordinate of the point where the common tangent touches $n_s(t_0)$. The value of $n_s(t_0)$ at this point is approximately $n_{s_0}(t_0) \sim t_0^{-2z}$. At $t=t_0+\Delta t$ we have $s_0(t_0+\Delta t) \sim (t_0+\Delta t)^z$ and $n_{s_0}(t_0+\Delta t) \sim (t_0+\Delta t)^{-2z}$. Calculating the slope of the straight line connecting these points on a double-logarithmic plot for $\Delta t \to 0$, we obtain, as the slope,

$$\mathscr{S} = \lim_{\Delta t \to 0} \frac{-2z \log_{10} t_0 + 2z \log_{10}(t_0+\Delta t)}{z \log_{10} t_0 - z \log_{10}(t_0+\Delta t)} = -2 \, .$$

Therefore, the scaling theory predicts the common slope to be equal to -2, in good agreement with the simulation results. The values of the exponents τ, w, and z, determined from various cases, are listed in Table I and satisfy the scaling relation $w=(2-\tau)z$.

Another way of testing the dynamic scaling is to plot $s^2 n_s(t)$ versus s/t^z. If Eq. (1) is valid, all results for a given γ must fall on one curve, which is the scaling function $f(x)$. In Fig. 4, plots of $n_s(t)$ for different times are scaled in this way into one universal scaling function. For $\gamma > -\frac{1}{2}$ the plots do not collapse so well (Fig. 5); however, the tendency that they would approach a single distribution for considerably larger times and cluster sizes can be seen. Unfortunately, this region cannot be studied due to the prohibitively large computer-time and -memory requirements.

Next we discuss the effect of a cluster-mass-dependent diffusion constant on the cluster-size distribution. The results presented in Sec. III show that the behavior of $n_s(t)$ is very nonuniversal as a function of γ, where the diffusivity of a cluster of size s is $D_s \sim s^{\gamma}$. For $\gamma \gg 1$ the large clusters move much faster, and relatively many small clusters remain intact during the process. If $\gamma \ll 1$ the speed of the small clusters is higher; therefore, these clusters die out by joining together and building up large clusters. From Figs. 1–5 we conclude that the exponents δ and z in the scaling form (1) change continuously as γ decreases. The dependence of z on γ has also been obtained from a mean-field–type approximation by Kolb,[31] giving reasonable agreement for some range of γ values. At a value of $\gamma=\gamma_c$, the behavior of the cluster-size distribution changes qualitatively and becomes nonmonotonic. Figure 6 shows cluster-size distribution functions obtained from some of our two-dimensional simulations of cluster-cluster aggregation with several values for the diffusivity exponent γ. The characteristic shapes of the cluster-size distribution function for $\gamma < \gamma_c$ and $\gamma > \gamma_c$ are different. There are, therefore, two main regimes ($\gamma < \gamma_c$ and $\gamma > \gamma_c$), and the results for $\gamma < \gamma_c$ can be represented by the scaling form (1) originally used for $\gamma > \gamma_c$,

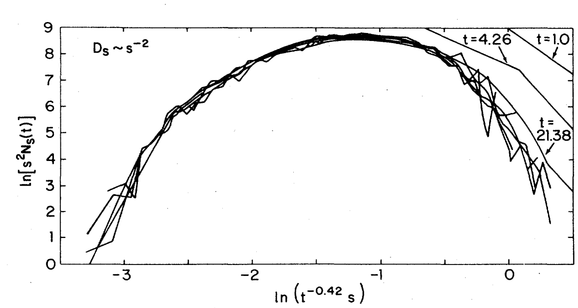

FIG. 4. Scaling of the time-dependent cluster-size distributions shown in Fig. 1(d). Except at short times, the scaled data fall on a single curve (the scaling function). The exponent z can be obtained directly from Figs. 1(a) and 1(b).

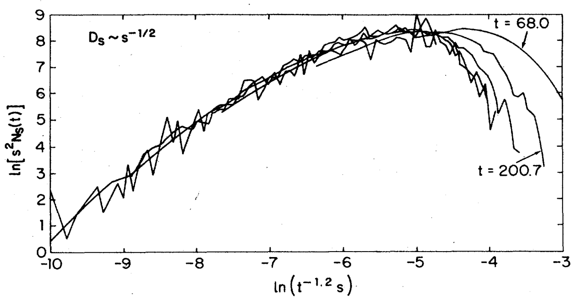

FIG. 5. Scaling of the time-dependent cluster-size distributions obtained from three-dimensional simulations with a diffusivity exponent $\gamma_c = -\frac{1}{2}$ and a particle concentration $\rho = 0.0034$. For this value of γ, the scaling procedure works well only at long times, and for $\gamma > -\frac{1}{2}$ the scaled curves do not coincide for simulations carried out on a practical scale.

$$n_s(t) \sim s^{-2}\tilde{f}(s/t^z),$$

with a different scaling function $\tilde{f}(x) \sim x^2 g(x)$, where $g(x)$ is a cutoff function for both the small and the large values of its argument, $g(x) \ll 1$ for $x \ll 1$ and $g(x) \ll 1$ for $x \gg 1$. In two dimensions ($d=2$), $\gamma_c \simeq -\frac{1}{4}$, while for $d=3$, $\gamma_c \simeq -\frac{1}{2}$. According to the Kirkwood-Riesman theory combined with simulation results,[33] the diffusion coefficient of three-dimensional cluster-cluster aggregation depends on the size of the clusters as $D_s \sim s^{-0.544}$. Therefore, γ_c is just in the range where γ is expected to be in a real system in which the diffusion process is controlled by the shear viscosity.

Besides γ, the cluster-size distribution may depend on other parameters in a realistic experiment. For example, a size-dependent sticking probability has a similar effect on n_s as an s-dependent diffusion constant.[34] Such details change the critical value of γ, and as a result, in the realistic experiments cluster-size distributions of both kinds have been observed. von Schulthess *et al.*[6] have found

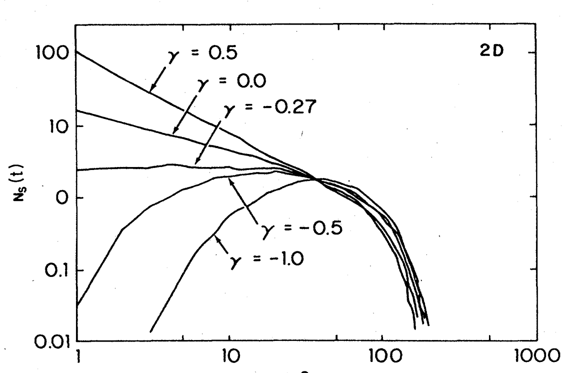

FIG. 6. Cluster-size distribution functions obtained from two-dimensional simulations of cluster-cluster aggregation on a 400^2 lattice with a density $\rho = 0.05$ for several values of the diffusivity exponent γ. As γ is decreasing, at a critical value of the diffusivity exponent $\gamma_c \simeq -\frac{1}{4}$, the monotonic decay of the cluster-size distribution crosses over into a different, bell-shaped behavior.

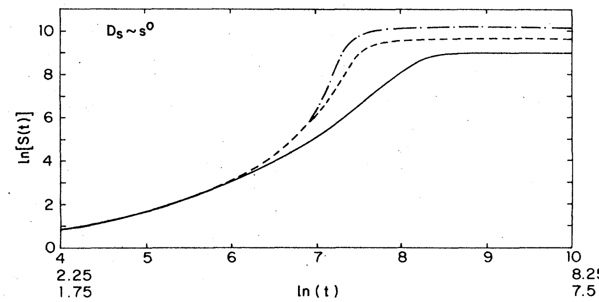

FIG. 7. Time dependence of the mean cluster size $S(t)$ obtained from three simulations of cluster-cluster aggregation at three different concentrations. In order to show the difference in the behavior of $S(t)$ for various concentrations more explicitly, the plots of the mean cluster size were shifted to make their short-time parts coincide. The three time intervals on which $S(t)$ is displayed are the following: for $\rho = 0.025$, $\ln(t_1) = 1.75$, and $\ln(t_2) = 7.5$ (dashed-dotted line); for $\rho = 0.015$, $\ln(t_1) = 2.25$, and $\ln(t_2) = 8.25$ (dashed line); and for $\rho = 0.0034$, $\ln(t_1) = 4.0$, and $\ln(t_2) = 10.0$ (solid line).

that $n_s(t)$ for antibody-antigen aggregation decays with a power law in s and t. In contrast, in the experiments on coagulation of air particulate,[4,5] aggregation of CO_2,[7] and aggregation of N_2O,[8] a bell-shaped cluster-size distribution has been found. A crossover from a monotonic decrease to a function with a maximum has been found in an analytic approach for $n_s(t)$.[30] However, the calculated value of γ_c differs from the simulation result.

The particle concentration is an important parameter in our simulations. We expect to find simple scaling behavior only in the limit of zero concentration. However, simulations at low particle concentrations require much more computer time to obtain results which are not subject to large statistical uncertainties. Since we have carried out simulations at several concentrations, we can be reasonably certain that our results are not subject to large finite-concentration effects. Figure 7 shows the time dependence of the mean cluster size $S(t)$ obtained from simulations carried out at densities of 0.0034, 0.015, 0.025. it can be seen from this figure that finite-concentration effects may be important even at concentrations as low as 0.015 or smaller. It should be noted, however, that the sensitivity to finite concentrations is much smaller for smaller values of γ.

Most theoretical and experimental studies in colloid science have been concerned with the behavior of dilute colloid dispersions. However, the particle concentration in many practical systems is much higher than that used in our simulations. A study of the kinetics of cluster-cluster aggregation at higher particle concentrations will be subject of future work.

V. CONCLUSIONS

In conclusion, we have reported the results of computer-simulation studies of the dynamic cluster-size distribution for the model of diffusion-limited aggregation of clusters. The results are found to be in agreement with the recent scaling theory, although the shape of the distribution function is nonuniversal, depending on the diffusion coefficient. These results are in qualitative agreement with the experiments, and we hope that appropriate data that could be quantitatively compared with our results will soon be available.

ACKNOWLEDGMENTS

The research conducted at Emory University was supported by grants from the Research Corporation, the Emory University Research Fund, and the National Science Foundation (Grant No. DMR-82-08051).

---

*On leave from Institute for Technical Physics, P.O. Box 76, Budapest, Hungary, H-1325.

[1]See, e.g., *Kinetics of Aggregation and Gelation,* edited by F. Family and D. P. Landau (North-Holland, Amsterdam, 1984).

[2]S. K. Friedlander, *Smoke, Dust and Haze: Fundamentals of Aerosol Behavior* (Wiley, New York, 1977).

[3]T. Vicsek and F. Family, Phys. Rev. Lett. **52**, 1669 (1984).

[4]R. B. Husar and K. T. Whitby, Environ. Sci. Technol. **7**, 241 (1973).

[5]G. Gartrell, Jr. and S. K. Friedlander, Atmos. Environ. **9**, 279 (1975).

[6]G. K. von Schulthess, G. B. Benedek, and R. W. de Blois, Macromolecules **13**, 939 (1980).

[7]J. M. Soler, N. Garcia, O. Echt, K. Sattler, and E. Recknagel, Phys. Rev. Lett. **49**, 1857 (1982).

[8]K. Sattler, in *Festkörperprobleme (Advances in Solid State Physics),* edited by P. Grosse (Vieweg, Braunschweig, 1983), Vol. XXIII, p. 1.

[9]M. von Smoluchowski, Z. Phys. Chem. **92**, 129 (1918); Z. Phys. **17**, 585 (1916).

[10]R. L. Drake, in *Topics in Current Aerosol Research,* edited by G. M. Hidy and J. R. Brock (Pergamon, New York, 1972), Vol. 3, 201.

[11]P. Meakin, Phys. Rev. Lett. **51**, 1119 (1983).

[12]M. Kolb, R. Botet, and R. Jullien, Phys. Rev. Lett. **51**, 1123 (1983).

[13]B. B. Mandelbrot, *The Fractal Geometry of Nature* (Freeman, San Franciso, 1982).

[14]T. A. Witten, Jr. and L. M. Sander, Phys. Rev. Lett. **47**, 1400 (1981).

[15]P. Meakin, Phys. Rev. B **29**, 4327 (1984); **29**, 3722 (1984).

[16]L. Niemeyer, L. Pietronero, and H. J. Weismann, Phys. Rev. Lett. **52**, 1033 (1984).

[17]K. Binder, Ann. Phys. (N.Y.) **98**, 390 (1976).

[18]D. Stauffer, Phys. Rep. **54**, 1 (1979).

[19]J. W. Essam, Rep. Prog. Phys. **43**, 833 (1980).

[20]K. Binder, Phys. Rev. B **15**, 4425 (1977).

[21]A. Chhabra, D. Matthews-Morgan, D. P. Landau, and H. J. Herrmann, in *Kinetics of Aggregation and Gelation,* Ref. 1, p. 39.

[22]Z. Rácz and T. Vicsek, Phys. Rev. Lett. **51**, 2382 (1983).

[23]T. Vicsek, J. Phys. A **16**, L647 (1983).

[24]Z. Djordevic (private communication).

[25]D. A. Weitz, J. S. Huang, M. Y. Lin, and J. Sung, Phys. Rev. Lett. **53**, 1657 (1984).

[26]R. M. Ziff, J. Stat. Phys. **23**, 241 (1980).

[27]F. Leyvraz and H. R. Tschudi, J. Phys. A **15**, 1951 (1982).

[28]E. M. Hendriks, M. H. Ernst, and R. M. Ziff, J. Stat. Phys. **31**, 519 (1983).

[29]F. Leyvraz, Phys. Rev. A **29**, 854 (1984).

[30]R. Botet and R. Jullien, J. Phys. A **17**, 2517 (1984).

[31]M. Kolb, Phys. Rev. Lett. **53**, 1653 (1984).

[32]T. Vicsek and F. Family, in *Kinetics of Aggregation and Gelation,* Ref. 1, p. 110.

[33]P. Meakin, Z. Y. Chen, and J. M. Deutch (unpublished).

[34]F. Family, P. Meakin, and T. Vicsek (unpublished).